

Synthesizing Diverse, High-Quality Audio Textures

Joe Antognini, Matt Hoffman, Ron J. Weiss

Abstract—Texture synthesis techniques based on matching the Gram matrix of feature activations in neural networks have achieved spectacular success in the image domain. In this paper we extend these techniques to the audio domain. We demonstrate that synthesizing diverse audio textures is challenging, and argue that this is because audio data is relatively low-dimensional. We therefore introduce two new terms to the original Grammian loss: an autocorrelation term that preserves rhythm, and a diversity term that encourages the optimization procedure to synthesize unique textures. We quantitatively study the impact of our design choices on the quality of the synthesized audio by introducing an audio analogue to the Inception loss which we term the VGGish loss. We show that there is a trade-off between the diversity and quality of the synthesized audio using this technique. We additionally perform a number of experiments to qualitatively study how these design choices impact the quality of the synthesized audio. Finally we describe the implications of these results for the problem of audio style transfer.

Index Terms—Machine learning, Audio, Texture synthesis

I. INTRODUCTION

Texture synthesis has been studied for over fifty years [1]. The problem is to take a sample of some textured data (usually an image) and generate synthesized data which have the same texture, but are not identical to the original sample. This problem is interesting as a machine learning problem in its own right, but successful texture synthesis methods can also elucidate the way in which humans perceive texture [2].

Portilla and Simoncelli [3] pioneered a very successful approach to image texture synthesis that tries to find a complete set of statistics that describe the perceptually relevant aspects of a given texture. To synthesize a new texture, a random input is perturbed until its statistics match those of the targets. Portilla and Simoncelli [3] developed a set of four classes of statistics consisting of 710 parameters which produced extremely realistic images of natural and synthetic textures. McDermott and Simoncelli [2] used a similar approach to develop four

classes of statistics in a cochlear model to synthesize textural audio spectrograms. This work produced convincing audio data for many natural audio textures (e.g., insects in a swamp, a stream, applause), but had difficulty with pitched and rhythmic textures (e.g., wind chimes, walking on gravel, church bells).

Gatys et al. [4] introduced an extremely successful technique that replaced hand-crafted statistics with Gram-matrix statistics derived from the hidden feature activations of a trained convolutional neural network (CNN). By perturbing a random input to match these Gram matrices, Gatys et al. [4] produced compelling textures that were far more complicated than those achieved by any earlier work.

Given the success of Gatys et al. [4] in the image domain relative to the hand-crafted approach of Portilla and Simoncelli [3], it is natural to ask whether a similar CNN-based strategy could be adapted to the audio domain to build on the hand-crafted approach of McDermott and Simoncelli [2]. Ulyanov and Lebedev [5] proposed just such an extension of the approach of [4] to audio. Their basic approach works fairly well on many of the 15 examples they consider, but (as we demonstrate in Sec. IV) it has some of the same failure modes as the approach of McDermott and Simoncelli [2].

In this work, we examine the causes of these problems, analyze why they are more serious in the audio domain than in the image domain, and propose techniques to fix them.

II. PRELIMINARIES AND ANALYSIS

We begin by defining a rigorous notion of “audio texture”. Borrowing from Portilla and Simoncelli [3], we define an audio texture to be an infinitely long stationary random process that follows an exponential-family (maximum-entropy) distribution defined by a set of local sufficient-statistic functions ϕ that are computed on patches of size M :

$$p_\lambda(x) \propto \exp\{\lambda^\top \sum_{t=0}^{\infty} \phi(x_{t,\dots,t+M})\}, \mathbb{E}_{p_\lambda}[\phi] = \bar{\phi}. \quad (1)$$

We only ever observe finite clips from this theoretically infinite signal. If an observed clip is long enough relative to M and the dimensionality of ϕ , then we can reliably estimate the expected sufficient statistics $\bar{\phi}$ from data.

Work done as a Google AI Resident

The first practical question we face is whether to model the data in the time domain (i.e., the raw waveform) or the frequency domain (via a spectrogram). Although direct time-domain modeling has seen enormous success in recent years with WaveNet [6], these autoregressive techniques are still slow to train and extremely computationally demanding at synthesis-time. Following Ulyanov and Lebedev [5], we instead use the spectrogram representation in this work. This incurs the disadvantage of needing to invert the spectrogram to recover audio with the Griffin-Lim algorithm [7], which can introduce artifacts, but is much faster and permits the unsupervised techniques we use in this work, eliminating the need to train a large model.

Naively, an audio spectrogram can be treated like a two-dimensional greyscale image, with time on one axis and frequency on the other. But in texture synthesis, it is more natural to treat frequency bins in an audio spectrogram as channels (analogous to RGB color channels in an image) rather than spatial dimensions. Audio textures are not stationary on the frequency axis—shifts in frequency tend to change the semantic meaning of a sound. Therefore, although the “spectrogram-as-image” interpretation can work well for some analysis problems [8], it is a poor fit to the assumptions underlying texture synthesis.

Treating spectrograms as one-dimensional multi-channel stationary signals raises an important statistical issue that is not as salient in image texture synthesis. Images typically have only three channels, whereas audio spectrograms have as many channels as there are samples in the FFT window divided by two (typically some power of two between 128 and 2048). Furthermore, the number of patches that are averaged to estimate the statistics that define the target texture distribution is on the order of the length of the signal, whereas in images the number of patches grows as the product of the dimensions. So in audio texture synthesis, we need to estimate a function of more channels with fewer observations, which may lead to overfitting. We indeed find that synthesizing diverse audio textures is more difficult than synthesizing diverse images and extra care must be taken to encourage diversity (with tongue planted in cheek, this may perhaps be called a curse of low dimensionality).

III. METHODS

A. Signal processing

We produce audio textures by transforming the target audio to a log spectrogram and synthesizing a new spectrogram. We then use the Griffin-Lim algorithm [7] to invert the spectrogram and generate the synthesized audio texture. If necessary, we resample the target audio to 16

kHz and normalize. We produce a spectrogram by taking the absolute value of the short-time Fourier transform with a Hann window of size 512 samples and a hop size of 64 samples. Although taking the absolute value removes any explicit phase information, if the hop size is less than or equal to half the window size phase information is implicitly retained (i.e., there exists a unique audio signal corresponding to such a spectrogram up to a global phase; [9]). We then add 1 to every magnitude in the spectrogram and take the natural logarithm. Adding 1 guarantees that the log-spectrogram is finite and positive.

B. Architecture of the neural networks

We obtained the best textures with a set of six single-hidden-layer random CNNs. Unlike the case of image texture synthesis, audio spectrograms are one-dimensional so we therefore use a one-dimensional convolution. Each CNN had a convolutional kernel with a different width, varying in powers of 2 from 2 to 64 frames. We applied a ReLU activation after the convolutional layers. Each layer had 512 filters randomly drawn using the Glorot initialization procedure [10]. Several authors have found that random convolutional layers perform as well as trained convolutional layers for image texture synthesis [11, 12]. Shu et al. [13] furthermore showed that a random CNN retains as much information to reconstruct an image as a trained convolutional network, if not more. Although we also tried synthesizing textures with an audio model that was trained on AudioSet [14], a dataset consisting of about one million 10 second audio clips with 527 labels, we did not find that this trained model produced textures that were any better than those produced by a random CNN.

Using an ensemble of CNNs with varying kernel sizes is crucial for obtaining high quality textures since each kernel size is most sensitive to audio features whose duration is comparable to the kernel size. The features of real-world audio can span many different timescales (e.g., just a few milliseconds for a clap and up to several seconds for a bell) so it is important to use an architecture which is sensitive to the range of timescales that is likely to be encountered. We consider the impact of our architecture design choices experimentally in Section IV-C.

C. Loss terms

The loss we minimize consists of three terms:

$$\mathcal{L} = \mathcal{L}_{\text{Gram}} + \alpha \mathcal{L}_{\text{autocorr}} + \beta \mathcal{L}_{\text{div}}. \quad (2)$$

The first term, $\mathcal{L}_{\text{Gram}}$, was introduced by Gatys et al. [4] and is intended to capture the average local correlations

between features in the texture. The second term, $\mathcal{L}_{\text{autocorr}}$, we adapt from Sendik and Cohen-Or [15] and is intended to capture rhythm. The final term, \mathcal{L}_{div} , we introduce to prevent the optimization process from exactly copying the original texture. The hyperparameters α and β are used to set the relative importance of these three terms. We find that $\alpha = 10^3$ and $\beta = 10^{-4}$ work well for many of the textures we studied, although hyperparameter tuning is sometimes required. In particular, highly rhythmic textures generally require a larger choice of α and a lower choice of β .

1) *Gram loss*: Let us write the features of the k th convolutional network as $F_{t\mu}^k$, where t indicates the position of a patch in the feature map (i.e., the time in the spectrogram), and μ indicates the filter. The Gram matrix for the k th convolutional network is the time-averaged outer product between the k th feature map with itself:

$$G_{\mu\nu}^k = \frac{1}{T} \sum_t F_{t\mu}^k F_{t\nu}^k, \quad (3)$$

where T is the number of windows in the spectrogram

We match this statistic by minimizing the Frobenius norm of the difference between the Gram matrices of the synthesized texture and the target for all layers and normalizing to the Frobenius norm of the target texture Gram matrix:

$$\mathcal{L}_{\text{Gram}} = \frac{\sum_{k,\mu,\nu} (G_{\mu\nu}^k - \tilde{G}_{\mu\nu}^k)^2}{\sum_{k,\mu,\nu} (\tilde{G}_{\mu\nu}^k)^2}. \quad (4)$$

Throughout this paper tilde denotes the target texture.

2) *Autocorrelation loss*: While minimizing the Gram loss alone produces excellent audio for many kinds of audio textures, we show in Sec. IV-B1 that the Gram loss fails to capture rhythm. To this end, we adapt a loss term introduced by Sendik and Cohen-Or [15] derived from the autocorrelation of the feature maps that was developed to capture periodic structure in image textures.¹ The autocorrelation of the k th feature map is

$$A_{\tau\mu}^k = \mathcal{F}_f^{-1} \left[\mathcal{F}_t[F_{t\mu}^k] \mathcal{F}_t[F_{t\mu}^k]^* \right], \quad (5)$$

where \mathcal{F}_t represents the discrete Fourier transform with respect to time t , $*$ represents complex conjugation, and τ represents the lag. The autocorrelation loss is the sum of the normalized Frobenius norms of the squared differences between the target and synthesized autocorrelation maps:

$$\mathcal{L}_{\text{autocorr}} = \frac{\sum_{k,\tau,\mu} (A_{\tau\mu}^k - \tilde{A}_{\tau\mu}^k)^2}{\sum_{k,\tau,\mu} (\tilde{A}_{\tau\mu}^k)^2}. \quad (6)$$

¹Note that Sendik and Cohen-Or [15] use a variant of the feature map autocorrelation called the structural matrix, but we find that the autocorrelation works well and is faster to compute.

We generally do not expect to encounter rhythmic structure on timescales longer than a few seconds, and autocorrelations on extremely short timescales (under 200 ms) are captured within the receptive fields of individual networks. Including very short and long lags in the loss tends to encourage overfitting without adding any useful rhythmic activity to the texture (this is particularly true for lags near 0 since the autocorrelation will always be largest there and will therefore be the largest contributor to $\mathcal{L}_{\text{autocorr}}$). For this reason we only sum over lags of 200 ms to 2 s.

3) *Diversity loss*: As we show in Sec. IV-B2, a downside of using the previous two loss terms alone is that they tend to reproduce the original texture exactly. Sendik and Cohen-Or [15] proposed a diversity term for image texture synthesis of the form

$$\mathcal{L}_{\text{Sendik}} = - \sum_{k,t,\mu} \left(F_{t\mu}^k - \tilde{F}_{t\mu}^k \right)^2, \quad (7)$$

which is maximized when the two feature maps match exactly. We found that this diversity term has two shortcomings: first, because this term can become arbitrarily negative, it can dominate the total loss and destabilize the optimization (see Fig. 1); second, we find that this loss has a tendency to reproduce the original input, but slightly shifted in time (see Fig. 2). To address these two issues, we propose the following shift-invariant diversity term:

$$\mathcal{L}_{\text{div}} = \max_s \left(\frac{\sum_{k,t,\mu} (\tilde{F}_{t\mu}^k)^2}{\sum_{k,t,\mu} (F_{t+s,\mu}^k - \tilde{F}_{t\mu}^k)^2} \right), \quad (8)$$

where the shift s can take on values ranging from 0 to $T - 1$. In other words, we compute the negative inverse of the diversity term of Eq. 7 for all possible relative shifts between the original and synthesized textures and then take the maximum. Since computing this loss for all possible shifts is computationally expensive, we compute this loss in steps of 50 frames, cycling through different sets of frames in each step of the optimization process, along with computing the loss for the shifts which yielded the largest loss in the last 10 optimization steps.

D. Optimization

We find that L-BFGS-B [16] works well to minimize the loss and obtain high quality audio textures. We optimized for 2000 iterations and used 500 iterations of the Griffin-Lim algorithm. We furthermore found it useful to include the diversity loss term for only the first 100 iterations; by this point the optimizer had found a nontrivial local optimum, and continuing to incorporate the diversity loss reduced texture quality. Spectrograms of four synthesized textures are shown in Fig. 3. We show the

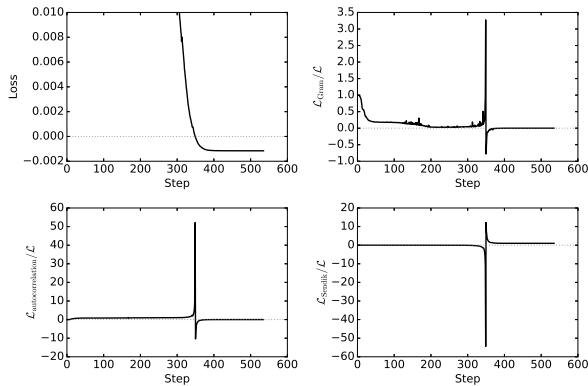


Fig. 1. The overall loss and the relative contributions of the three components during optimization of a wind chimes texture using $\mathcal{L}_{\text{Sendik}}$ instead of \mathcal{L}_{div} . This diversity term can lead to negative losses, which in turn makes optimization difficult when the loss passes through zero. In part to avoid these instabilities we propose a diversity term of the form Eq. 8.

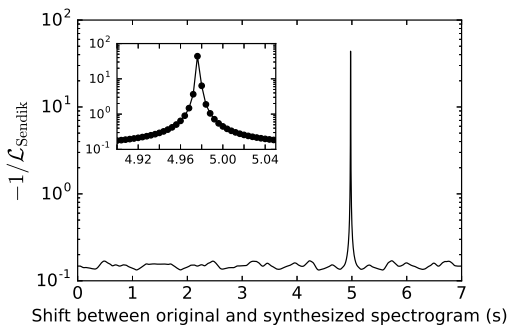


Fig. 2. The inverse negative diversity term used by Sendik and Cohen-Or [15] as a function of a synthesized texture shifted in time. The synthesized texture closely matches the original texture, but is shifted in time by about five seconds. $\mathcal{L}_{\text{Sendik}}$ fails to capture this effect as demonstrated by the sharp peak. Inset zooms in on the peak to show that the peak is resolved.

relative values of the various loss terms during optimization in Fig. 4. Corresponding audio for all spectrograms, along with supplementary information, can be found at https://antognini-google.github.io/audio_textures/.

IV. EXPERIMENTS

A. Quantitative evaluation of texture quality

Quantitatively evaluating the quality of generative models is difficult. Salimans [17] developed a useful quantitative metric for comparing generative adversarial networks based on the Kullback-Liebler divergence of the label predictions given by the Inception classifier [18] between the sampled images and the original dataset. We adapt this “Inception score” to assess the quality of our audio textures compared to other methods. Rather than

Inception, we use the “VGGish” CNN² that was trained on AudioSet.³ The motivation for our “VGGish score” is that the label predictions produced by the VGGish model should match between the original and synthesized textures. To this end, we define the score as

$$\mathcal{S}_{\text{VGGish}} \equiv \exp [\mathbb{E}_x [\text{KL} (p_{\text{VGGish}}(y|\tilde{x}) || p_{\text{VGGish}}(y|x))]], \quad (9)$$

where y represents the VGGish label predictions and x represents the texture audio. We compute $\mathcal{S}_{\text{VGGish}}$ over the 168 textures used by McDermott and Simoncelli [2]. These textures span a broad range of sound, including natural and artificial sounds, pitched and non-pitched sounds, and rhythmic and non-rhythmic sounds. We compare this VGGish score between our models optimized with different loss terms and the approaches used by Ulyanov and Lebedev [5] and McDermott and Simoncelli [2] in Table I, separating out the scores for pitched and rhythmic textures. We also compare an autocorrelation score and a diversity score computed from the generated spectrograms discussed in Sections IV-B1 and IV-B2, respectively.

The best VGGish scores are obtained by using $\mathcal{L}_{\text{Gram}}$ alone. As expected, adding $\mathcal{L}_{\text{autocorr}}$ substantially reduces the autocorrelation score, though at the cost of increasing the diversity score, and adding a larger weight to \mathcal{L}_{div} generally reduces the diversity score. The lowest diversity scores are obtained by McDermott and Simoncelli [2], though at the cost of substantially higher autocorrelation scores and relatively large VGGish scores for pitched textures.

It is unsurprising that adding \mathcal{L}_{div} reduces the VGGish score because introducing any diversity will generally reduce the VGGish score (the model could achieve a perfect VGGish score simply by copying the original input). It is, however, surprising that adding $\mathcal{L}_{\text{autocorr}}$ alone also reduces the VGGish score. Although introducing $\mathcal{L}_{\text{autocorr}}$ qualitatively seems to increase overfitting, this overfitting occurs on very long timescales (i.e., the model will reproduce several seconds that sound very similar to the original audio). Introducing $\mathcal{L}_{\text{autocorr}}$ seems to make the optimization process more difficult for timescales much shorter than the minimum lag considered by $\mathcal{L}_{\text{autocorr}}$, which leads to lower quality on short timescales and thus higher VGGish scores.

²Available from <https://github.com/tensorflow/models/tree/master/research/audioset>.

³VGGish produces 128 dimensional embeddings rather than label predictions. To obtain label predictions we trained a set of 527 logistic regression classifiers on top of the AudioSet embeddings (AudioSet’s 527 classes are not mutually exclusive.) We trained for 100,000 steps with a learning rate of 0.1 and achieved a test accuracy of 99.42% and a test cross entropy loss of 0.0584.

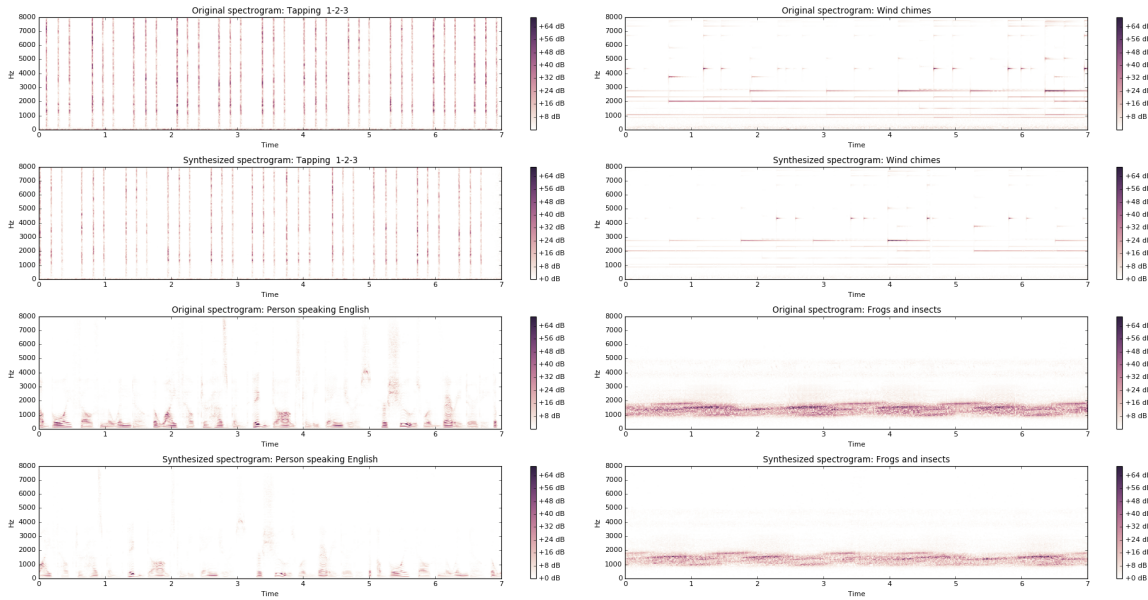


Fig. 3. Four pairs of synthesized audio textures with the originals. These textures include pitched audio (wind chimes, upper right), rhythmic audio (tapping, upper left), speech (lower left), and natural sounds (lower right).

TABLE I
A COMPARISON OF SCORES BETWEEN OUR MODEL AND OTHER WORK.

	VGGish ($\times 10^{-4}$)			Autocorrelation			Diversity		
	Rthm.	Ptch.	Other	Rthm.	Ptch.	Other	Rthm.	Ptch.	Other
Spectrograms recovered via Griffin-Lim	9.7	12.6	7.1	7.4	0.54	2.9	21.4	29.7	22.7
McDermott and Simoncelli [2]	16.7	33.2	8.3	542.0	408.1	421.9	1.6	1.6	2.0
Ulyanov and Lebedev [5]	13.4	26.8	10.0	40.6	23.3	27.4	2.9	3.0	3.3
$\mathcal{L}_{\text{Gram}}$	9.9	16.8	7.3	29.0	9.7	6.5	2.4	3.0	3.5
$\mathcal{L}_{\text{Gram}} + \mathcal{L}_{\text{autocorr}}$	17.8	21.3	17.9	13.3	7.4	15.6	3.4	5.4	5.0
$\mathcal{L}_{\text{Gram}} + \mathcal{L}_{\text{autocorr}} + \mathcal{L}_{\text{div}} (\beta = 10^{-5})$	14.5	23.0	12.2	13.0	2.3	7.2	3.8	6.8	4.4
$\mathcal{L}_{\text{Gram}} + \mathcal{L}_{\text{autocorr}} + \mathcal{L}_{\text{div}} (\beta = 10^{-3})$	14.9	19.0	10.0	4.7	3.7	7.1	5.0	4.9	3.9

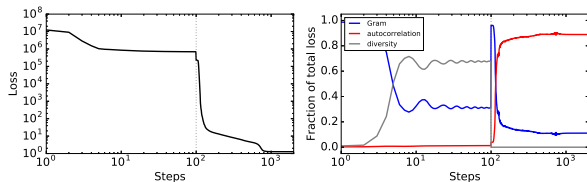


Fig. 4. Left panel: loss during optimization of the wind chimes texture. Right panel: the fraction of the total loss each of the three terms contributes during optimization.

B. Effect of the different loss terms

1) *Autocorrelation loss*: To demonstrate the necessity of $\mathcal{L}_{\text{autocorr}}$ we synthesize textures with a variety of values of α . For simplicity we set $\beta = 0$ in these experiments (i.e., we exclude \mathcal{L}_{div} from the total loss). We show spectrograms for a highly rhythmic tapping texture using two different values of α in Fig. 5. If

the weight of $\mathcal{L}_{\text{autocorr}}$ is small, the synthesized textures reproduce tapping sounds which lack the precise rhythm of the original. Only when α is sufficiently large is the rhythm reproduced. We further demonstrate that minimizing $\mathcal{L}_{\text{autocorr}}$ reproduces rhythms by showing in Fig. 6 the autocorrelation functions of the spectrograms of a rhythmic and non-rhythmic texture.⁴ We furthermore compute the squared loss between the autocorrelation of each synthesized texture and its target texture, normalized to the Frobenius norm of the autocorrelation of the target texture. We present these scores in Table I. Qualitatively we find that, as expected, $\mathcal{L}_{\text{autocorr}}$ is most important in textures with substantial rhythmic activity and so it is useful to use a relatively large value for α for these rhythms. For textures without substantial rhythmic activity we find that a smaller choice of α produces higher quality

⁴Note that this is *not* directly minimized by minimizing Eq. 6 which is a function of the CNN features, not the spectrogram itself.

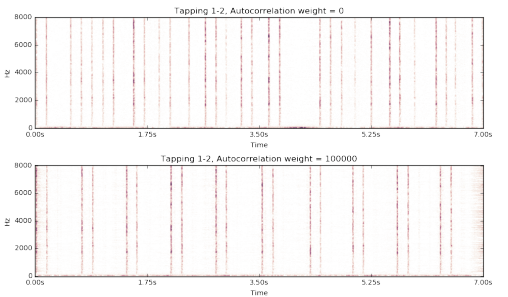


Fig. 5. Spectrograms of a rhythmic tapping texture synthesized with different weights for $\mathcal{L}_{\text{autocorr}}$. Rhythm is only reproduced when the weight on $\mathcal{L}_{\text{autocorr}}$ is sufficiently large.

textures.

2) *Diversity loss*: To demonstrate the effect of \mathcal{L}_{div} we synthesize textures with a variety of values of β , keeping α fixed to 10^3 . We show in Fig. 7 spectrograms synthesized with two different values of β for two highly structured textures: wind chimes and speech. Smaller values of β generally reproduce the original texture but shifted in time (about 2 s for the wind chimes and about 3.25 s for speech). Larger values of β produce spectrograms which are not simple translations of the original input, but the quality of the resulting audio is much lower. In the case of the wind chimes the chimes do not have the hard onset in the original, and in the case of speech the voice is echoey and superimposes different phonemes. This is an instance of a more general diversity-quality trade-off in texture synthesis. In Fig. 8 we show the VGGish score (a rough proxy for texture quality) vs. the weight on the diversity term. As the weight on the diversity term increases, the average quality decreases. We furthermore calculate the diversity score on the spectrograms themselves to get a diversity score and present these scores in Table I.

We find that it is crucial to tune the loss weights for different texture classes in order to obtain the highest quality textures. Large α and large β , for example, is especially important for reliably generating rhythmic textures. Pitched audio generally requires a smaller choice of α and β . For non-textured audio like speech and music, high quality audio is only obtained with a large α and small β , which will only reproduce the original with some shift; since these kinds of audio do not obey the assumptions set out in Section II, any set of weights that does not reproduce the original will produce low quality audio.

C. Neural network architecture

The receptive field size of the convolutional kernel has a strong effect on the quality and diversity of the

synthesized textures. We show in Fig. 9 the effect of changing the receptive field size for two textures. To do this, we use the same set of single layer CNNs with exponentially increasing kernel sizes, but varying the maximum kernel size from 2 frames to 8. CNNs with very small receptive fields produce novel, but poor-quality textures that fail to capture long-range structure. Networks with large receptive fields tend to reproduce the original. This is an example of the quality-diversity trade-off in texture synthesis.

Another design choice we consider is the number of filters in the each network. We show in Fig. 10 the results of using 32, 128, and 512 filters to synthesize two textures. Note that because there are six CNNs in all with varying kernel sizes, the total number of activations varies from 192 to 3072. At least 128 filters are necessary to get reasonable textures, but the quality continues to improve with 512 filters.

We considered stacking six convolutional layers on top of each other, each with a receptive field of 2 and separated by an average pooling layer with a pool size of 2 and a stride of 2. This network has the same distribution of receptive field sizes as the six separate networks, but the input to each layer here must pass through the (random) filters of all the earlier layers. We compare spectrograms generated with this network to the six separate networks that we use elsewhere in Fig. 11. The only effect of stacking the layers is a modest degradation in the quality of long-range sounds, best seen in the wind chimes texture.

V. DISCUSSION

A. Towards compelling audio style transfer

After Gatys et al. [4] developed the Gram-based approach for texture synthesis, a natural extension was to propose a similar technique for artistic style transfer [19] in which there is an additional content term in the loss which is minimized by matching the high-level features of a second image. There have now been a variety of impressive results for image style transfer [20, 21, 22]. There have been a few attempts to extend these techniques to audio style transfer [5, 23, 24], and while the results are plausible, they are underwhelming compared to the results in the image domain. What makes the audio domain so much more challenging?

The first issue is that it is unclear what is meant by “style transfer.” The simplest form of style transfer would be to take a melody played on one instrument and make it sound as though it were played on another; or similarly voice conversion, i.e., taking audio spoken by one person and making it sound as though it had been

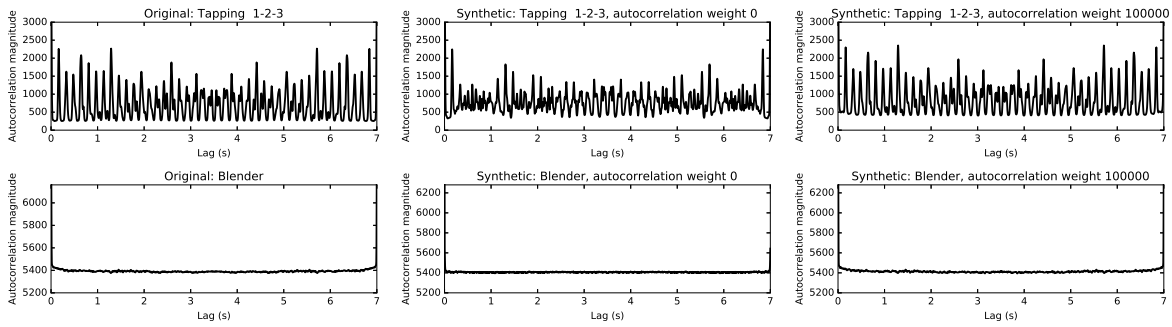


Fig. 6. Autocorrelation functions of a rhythmic (top row) and non-rhythmic (bottom row) texture for the original (left column) and two weights on $\mathcal{L}_{\text{autocorr}}$. Whereas the non-rhythmic texture has a flat autocorrelation function, the autocorrelation function of the rhythmic texture displays structure that is reproduced only when the weight on $\mathcal{L}_{\text{autocorr}}$ is large.

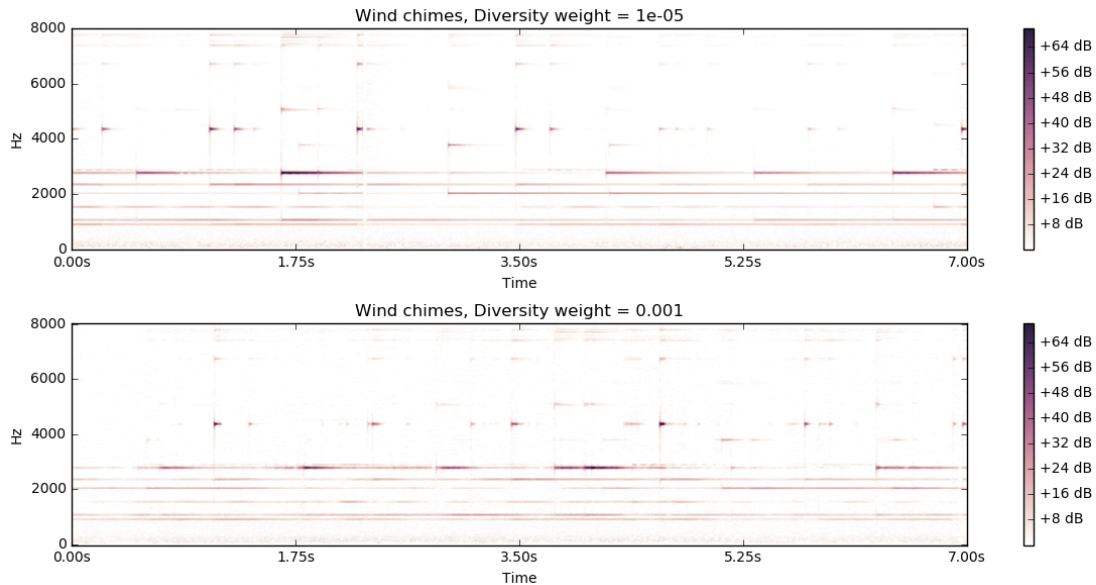


Fig. 7. Spectrograms synthesized with different weights β on \mathcal{L}_{div} for two non-stationary sounds: wind chimes (left) and speech (right).

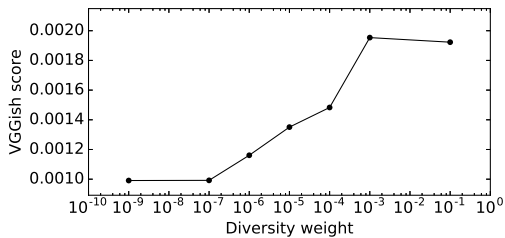


Fig. 8. The diversity-quality trade-off in texture synthesis. The VGGish score is a rough proxy for texture quality, with lower scores representing higher quality textures. As the diversity weight increases, the average quality of the textures decreases.

spoken by another [25]. While this simpler version of style transfer is still an open problem, the more interesting and far more difficult form of style transfer would be taking a melody from one genre (e.g., a Mozart aria) and

transforming it into one from another (e.g., a jazz song) by keeping the broad lyric and melodic structure, but replacing the instrumentation, ornamentation, rhythmic patterns, etc., characteristic of one genre with those of another. It is plausible that the simpler form of style transfer can be accomplished with careful design choices in the convolutional architecture [25]. But it does not appear that such an approach can work for the more complicated kind of style transfer.

To understand why, it is worth comparing the features learned by deep CNNs trained on image vs. audio data. In the image domain there is a well defined feature hierarchy, with lower layers learning simple visual patterns like lines and corners, and later layers learning progressively more complicated and abstract features like dog faces and automobiles in the final layers [26]. By contrast, CNNs in the audio domain have been far less studied.

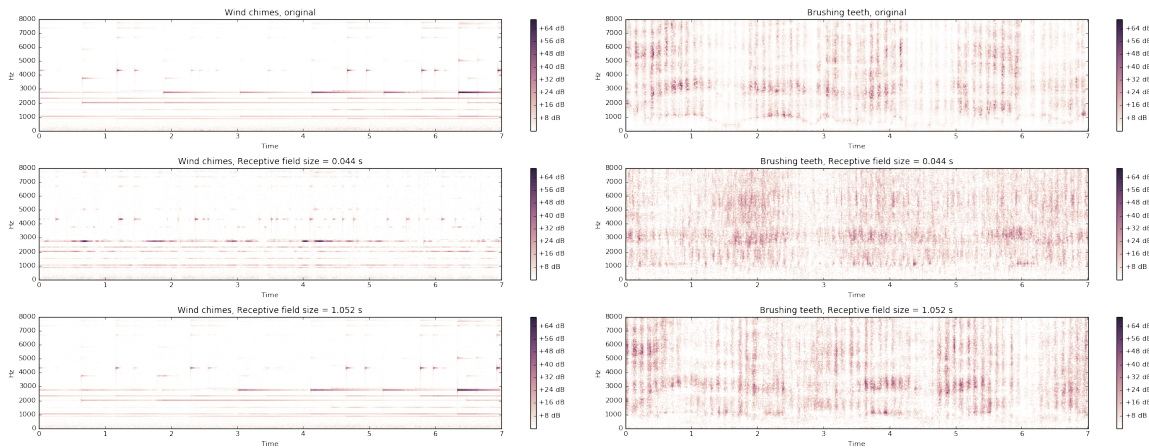


Fig. 9. Spectrograms synthesized from convolutional networks with different maximum receptive field sizes.

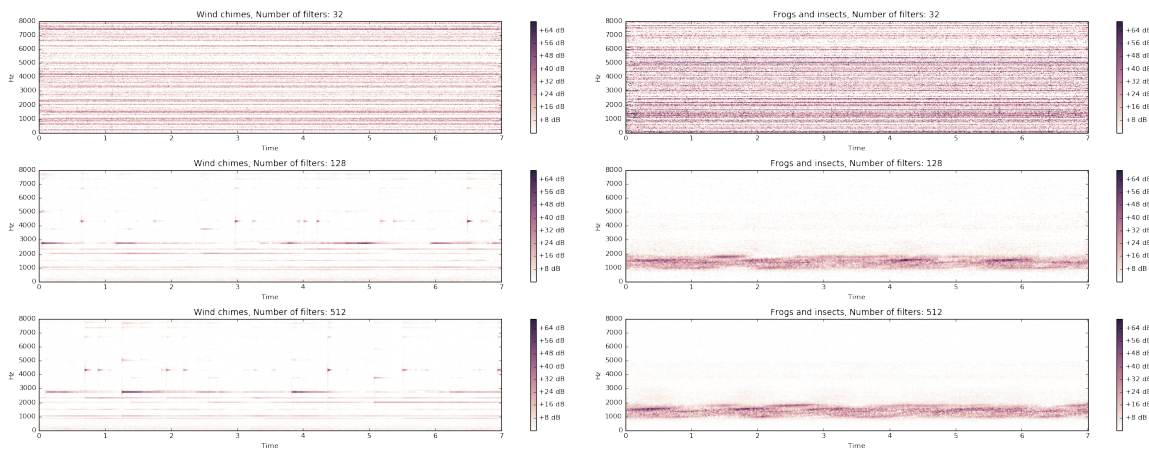


Fig. 10. Spectrograms for two textures synthesized with varying numbers of filters in the convolutional layers. With 32 filters, the textures have isolated power in some frequencies and not others, but have not developed any temporal structure. It is not until there are 128 filters that the textures introduce sounds that vary over time. However, for complex textures like wind chimes, only 512 filters are sufficient to produce the hard onsets of bells. See Fig. 3 for the originals.

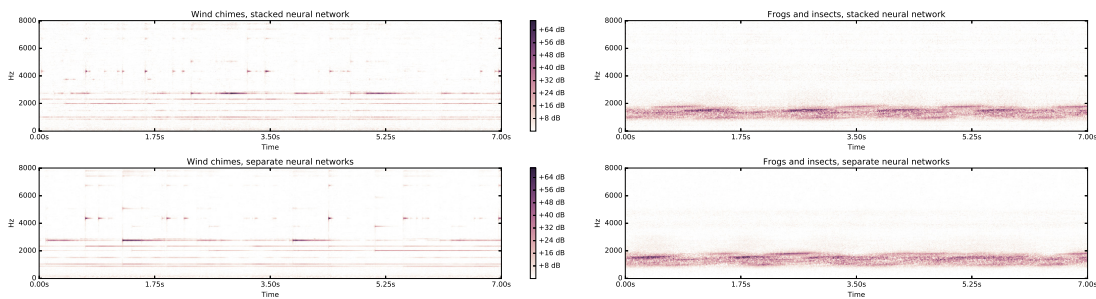


Fig. 11. Spectrograms for two textures synthesized with a neural network that consists of six convolutional layers stacked on top of each other, each with a receptive field size of 2 frames and separated by average pooling layers with a pooling size of 2 and a stride of 2. We compare these spectrograms to spectrograms synthesized with the six separate neural networks of varying receptive field sizes used elsewhere in this paper. The distribution of receptive field sizes in both neural networks is the same. See Fig. 3 for the originals.

Dieleman [27] analyzed patterns in the feature activations of a deep CNN trained on one million songs from the Spotify corpus in van den Oord [28]. Dieleman [27] found that features in lower layers identified local stylistic and melodic features, e.g., vibrato singing, vocal thirds, and bass drum. Features in later layers identified specific genres, e.g., Christian rock and Chinese pop. Whereas in the image domain the feature activations of the higher layers represent the content of the image (e.g., there is a dog in the lower left corner), in the audio domain the later layers instead represent the overall style. These differences reflect the way that these CNNs are trained. In the image domain, CNNs are explicitly trained to identify the content of the image. In the audio domain the CNN is instead trained to identify the overall style. This poses a challenge for style transfer because the “content” of the audio consists of the melody and lyrics, but the CNN is never trained to identify the content and so it either gets mixed in with other low-level textural features or is not propagated to later layers at all. Successful audio style transfer will require a network that can separate the melodic content of audio from its stylistic content the way that image classification CNNs can. The path forward may instead lie with neural networks trained on transcription or Query by Singing/Humming tasks.

VI. CONCLUSIONS

We have demonstrated that the approach to texture synthesis described by Gatys et al. [4] of matching Gram matrices from convolutional networks can be extended to the problem of synthesizing audio textures. There are, however, certain differences in the audio domain vs. the image domain that require the addition of two more loss terms to produce diverse, robust audio textures: an autocorrelation term to preserve rhythm, and a diversity term to encourage the synthesized textures to not exactly reproduce the original texture. We test our technique across several classes of textures like rhythmic and pitched audio and find that tuning the weights on the autocorrelation and diversity terms is crucial to obtaining the highest quality textures for different classes. The choice of architecture is also important to obtain high quality textures; an ensemble random convolutional neural networks with a wide range of receptive field sizes allows the model to capture features that occur on timescales across many orders of magnitude. Finally, we show that this method has a trade-off between the diversity and the quality of the results.

ACKNOWLEDGMENTS

The authors are grateful to Josh McDermott for providing the synthesized textures using the technique of

McDermott and Simoncelli [2] for comparison with the technique in this paper. The authors thank Rif A. Saurous for helpful comments on the manuscript.

REFERENCES

- [1] B. Julesz, “Visual pattern discrimination,” *IRE Transactions on Information Theory*, vol. 8, no. 2, pp. 84–92, 1962.
- [2] J. H. McDermott and E. P. Simoncelli, “Sound texture perception via statistics of the auditory periphery: evidence from sound synthesis,” *Neuron*, vol. 71, no. 5, pp. 926–940, 2011.
- [3] J. Portilla and E. P. Simoncelli, “A parametric texture model based on joint statistics of complex wavelet coefficients,” *International Journal of Computer Vision*, vol. 40, no. 1, pp. 49–70, 2000.
- [4] L. Gatys, A. S. Ecker, and M. Bethge, “Texture synthesis using convolutional neural networks,” in *Advances in Neural Information Processing Systems*, 2015, pp. 262–270.
- [5] D. Ulyanov and V. Lebedev, “Audio texture synthesis and style transfer,” 2016. [Online]. Available: <https://dmitryulyanov.github.io/audio-texture-synthesis-and-style-transfer/>
- [6] A. v. d. Oord, S. Dieleman, H. Zen, K. Simonyan, O. Vinyals, A. Graves, N. Kalchbrenner, A. Senior, and K. Kavukcuoglu, “WaveNet: A generative model for raw audio,” *arXiv preprint arXiv:1609.03499*, 2016.
- [7] D. Griffin and J. Lim, “Signal estimation from modified short-time fourier transform,” *IEEE Transactions on Acoustics, Speech, and Signal Processing*, vol. 32, no. 2, pp. 236–243, 1984.
- [8] S. Hershey, S. Chaudhuri, D. P. W. Ellis, J. F. Gemmeke, A. Jansen, R. C. Moore, M. Plakal, D. Platt, R. A. Saurous, B. Seybold, M. Slaney, R. J. Weiss, and K. Wilson, “CNN architectures for large-scale audio classification,” in *IEEE ICASSP*, Mar. 2017.
- [9] N. Sturmel and L. Daudet, “Signal reconstruction from STFT magnitude: A state of the art,” in *International Conference on Digital Audio Effects*, 2011.
- [10] X. Glorot and Y. Bengio, “Understanding the difficulty of training deep feedforward neural networks,” in *Proceedings of the Thirteenth International Conference on Artificial Intelligence and Statistics*, 2010, pp. 249–256.
- [11] K. He, Y. Wang, and J. Hopcroft, “A powerful generative model using random weights for the deep image representation,” in *Advances in Neural Information Processing Systems*, 2016, pp. 631–639.

- [12] I. Ustyuzhaninov, W. Brendel, L. A. Gatys, and M. Bethge, "Texture synthesis using shallow convolutional networks with random filters," *arXiv preprint arXiv:1606.00021*, 2016.
- [13] Y. Shu, M. Zhu, K. He, J. Hopcroft, and P. Zhou, "Understanding deep representations through random weights," *arXiv preprint arXiv:1704.00330*, 2017.
- [14] J. F. Gemmeke, D. P. Ellis, D. Freedman, A. Jansen, W. Lawrence, R. C. Moore, M. Plakal, and M. Ritter, "Audio set: An ontology and human-labeled dataset for audio events," in *IEEE ICASSP*, 2017.
- [15] O. Sendik and D. Cohen-Or, "Deep correlations for texture synthesis," *ACM Transactions on Graphics (TOG)*, vol. 36, no. 5, p. 161, 2017.
- [16] C. Zhu, R. H. Byrd, P. Lu, and J. Nocedal, "Algorithm 778: L-BFGS-B: Fortran subroutines for large-scale bound-constrained optimization," *ACM Transactions on Mathematical Software (TOMS)*, vol. 23, no. 4, pp. 550–560, 1997.
- [17] T. Salimans, I. Goodfellow, W. Zaremba, V. Cheung, A. Radford, and X. Chen, "Improved techniques for training GANs," in *Advances in Neural Information Processing Systems*, 2016, pp. 2234–2242.
- [18] C. Szegedy, W. Liu, Y. Jia, P. Sermanet, S. Reed, D. Anguelov, D. Erhan, V. Vanhoucke, A. Rabinovich *et al.*, "Going deeper with convolutions," in *CVPR*, 2015.
- [19] L. A. Gatys, A. S. Ecker, and M. Bethge, "A neural algorithm of artistic style," *arXiv preprint arXiv:1508.06576*, 2015.
- [20] T. Q. Chen and M. Schmidt, "Fast Patch-based Style Transfer of Arbitrary Style," *ArXiv e-prints*, Dec. 2016.
- [21] V. Dumoulin, J. Shlens, M. Kudlur, A. Behboodi, F. Lemic, A. Wolisz, M. Molinaro, C. Hirche, M. Hayashi, E. Bagan *et al.*, "A learned representation for artistic style," *arXiv preprint arXiv:1610.07629*, 2016.
- [22] D. Ulyanov, V. Lebedev, A. Vedaldi, and V. S. Lempitsky, "Texture networks: Feed-forward synthesis of textures and stylized images." in *ICML*, 2016, pp. 1349–1357.
- [23] E. Grinstein, N. Duong, A. Ozerov, and P. Perez, "Audio style transfer," *arXiv preprint arXiv:1710.11385*, 2017.
- [24] S. Barry and Y. Kim, "“Style” transfer for musical audio using multiple time-frequency representations," 2018. [Online]. Available: <https://openreview.net/forum?id=BybQ7zWCb>
- [25] J. Chorowski, R. J. Weiss, R. A. Saurous, and S. Bengio, "On using backpropagation for speech texture generation and voice conversion," *arXiv preprint arXiv:1712.08363*, 2017.
- [26] C. Olah, A. Mordvintsev, and L. Schubert, "Feature visualization," *Distill*, vol. 2, no. 11, p. e7, 2017.
- [27] S. Dieleman, "Recommending music on spotify with deep learning," 2014. [Online]. Available: <http://benanne.github.io/2014/08/05/spotify-cnns.html>
- [28] A. Van den Oord, S. Dieleman, and B. Schrauwen, "Deep content-based music recommendation," in *Advances in Neural Information Processing Systems*, 2013, pp. 2643–2651.



Joseph M. Antognini is a Google AI resident. At Google he has worked on applying machine learning to audio synthesis and studying the foundations of machine learning. He received his Ph.D. in astronomy from The Ohio State University in 2016.



Matthew D. Hoffman is a senior research scientist at Google. His main research focus is in probabilistic modeling and approximate inference algorithms. He has worked on various applications including music information retrieval, speech enhancement, topic modeling, learning to rank, computer vision, user interfaces, user behavior modeling, social network analysis, digital imaging, and astronomy. He is a co-creator of the widely used statistical modeling package Stan.



Ron J. Weiss is a software engineer at Google where he has worked on content-based audio analysis, recommender systems for music, and noise robust speech recognition. Ron completed his Ph.D. in electrical engineering from Columbia University in 2009 where he worked in the Laboratory for the Recognition of Speech and Audio. From 2009 to 2010 he was a postdoctoral researcher in the Music and Audio Research Laboratory at New York University.